

2. A. P. Farrell and D. J. Randall, *Can. J. Zool.* **56**, 939 (1978).
3. P. H. Greenwood and K. F. Liem, *J. Zool. London* **203**, 411 (1984).
4. J. P. Lomholt, K. Johansen, G. M. O. Maloiy, *Nature* **257**, 787 (1975).
5. C. Gans, *Forma Functio* **3**, 61 (1970).
6. Polypterid fishes have small heads in relation to their long bodies and lungs. The volume of air that buccal pumping can contribute to total ventilation is limited by the size of the buccal cavity. Volumes estimated from x-ray films combined with silicone casts of fresh specimens indicate that the maximum possible percentage of ventilation from buccal pumping is  $24 \pm 3\%$  in *Erpetoichthys calabaricus* and  $40 \pm 5\%$  in *Polypterus senegalus* ( $\pm 1$  standard deviation,  $n = 3$  specimens of each species). With an elliptic cylinder as a model for the lungs, a rough calculation on the *Polypterus* air-breath in Fig. 1 shows that for an increase in the minor axis of the ellipse from 4 to 8 mm due to aspiration and from 8 to 10 mm due to buccal air, the contribution from buccal pumping is approximately 30%.
7. A. M. Abdel Magid, *Anim. Behav.* **14**, 530 (1966); *Nature* **215**, 1096 (1967); J. S. Budgett, *Proc. Zool. Soc. London* **15**, 323 (1901).
8. J. B. West, *Respiratory Physiology—The Essentials* (Williams & Wilkins, Baltimore, ed. 2, 1979).
9. E. L. Brainerd and K. F. Liem, unpublished data.
10. D. M. Pearson, *Zool. J. Linn. Soc.* **72**, 93 (1981).
11. Polypterid fishes do not have ribs surrounding the body cavity; their only ribs are dorsal ribs that do not extend ventrad below the lateral line (10). Since deformation during exhalation occurs in the belly, it seems unlikely that the ribs are involved in storing energy for recoil aspiration. The ribs may, however, be involved in stiffening the body laterally, thus allowing only dorsoventral deformation. Manipulation of unpreserved, dead specimens shows no tendency for recoil in the body wall after the integument has been removed. Passive recoil of the scale jacket was observed by compressing live and slightly anesthetized polypterids. Deeply anesthetized and dead specimens have no muscle tonus and thus become soft and flaccid. Recoil was observed in dead specimens, however, when pressure was applied to the sides of the specimen to hold the scale jacket in its natural alignment.
12. D. J. Randall, in *The Biology of Lampreys*, M. W. Hardisty and I. C. Potter, Eds. (Academic Press, London, 1972), vol. 2.
13. A. S. Romer, *Vertebrate Paleontology* (Univ. of Chicago Press, Chicago, 1966).
14. J. L. van Leeuwen and M. Muller, *Neth. J. Zool.* **33**, 425 (1983).
15. We thank F. A. Jenkins for his help and support throughout this work, E. Otten for discussions on energy storage, and C. Gans and D. Carrier for discussions on ventilation mechanics. Thanks to L. Meszoly for preparing Fig. 3 and to H. S. Kim and E. H. Wu for assistance with some of the experiments. Supported by an NSF grant to K.F.L.

11 July 1989; accepted 26 October 1989

## The Anticodon Contains a Major Element of the Identity of Arginine Transfer RNAs

LADONNE H. SCHULMAN AND HEIKE PELKA

The contribution of the anticodon to the discrimination between cognate and noncognate tRNAs by *Escherichia coli* Arg-tRNA synthetase has been investigated by in vitro synthesis and aminoacylation of elongator methionine tRNA ( $\text{tRNA}_{\text{m}}^{\text{Met}}$ ) mutants. Substitution of the Arg anticodon CCG for the Met anticodon CAU leads to a dramatic increase in Arg acceptance by  $\text{tRNA}_{\text{m}}^{\text{Met}}$ . A nucleotide (A20) previously identified by others in the dihydrouridine loop of  $\text{tRNA}_{\text{m}}^{\text{Arg}}$ s makes a smaller contribution to the conversion of  $\text{tRNA}_{\text{m}}^{\text{Met}}$  identity from Met to Arg. The combined anticodon and dihydrouridine loop mutations yield a  $\text{tRNA}_{\text{m}}^{\text{Met}}$  derivative that is aminoacylated with near-normal kinetics by the Arg-tRNA synthetase.

THE MOLECULAR BASIS OF THE AMINO acid acceptor identity of tRNAs is still largely unknown, although progress has recently been made in determining structural features (identity elements) important for recognition of a number of *Escherichia coli* and yeast tRNAs by cognate aminoacyl-tRNA synthetases (1–11). Both biochemical and genetic experiments have indicated that the anticodon plays a role in defining the amino acid that will be attached to many tRNAs [reviewed in (1) and (12)]. However, the relative contribution of this sequence to tRNA identity has only been established in a few cases (2, 11).

Treatment of  $\text{tRNA}_{\text{m}}^{\text{Arg}}$  (ICG) (the major Arg isoacceptor tRNA in *E. coli* having the

anticodon ICG; I is inosine) with sodium bisulfite has been reported to result in loss of Arg acceptor activity by conversion of the anticodon base C35 to U35 (13). Chemical modification of G36 with ketoxal also inhibits aminoacylation of  $\text{tRNA}_{\text{m}}^{\text{Arg}}$  (ICG) (14), although modification of I34 with acetone-trile has no effect on recognition of the tRNA by Arg-tRNA synthetase (ArgRS) (15). Genetic experiments have shown that conversion of  $\text{tRNA}_{\text{m}}^{\text{Arg}}$  (ICG) into an amber suppressor tRNA having the anticodon CUA results in partial loss of Arg activity and insertion of mostly Lys into protein at the site of amber codons (1, 8). These results indicate an important role for one or more anticodon bases in selection of tRNA substrates by ArgRS.

A composite structure of the nucleotides common to the primary sequences (16) of

four *E. coli*  $\text{tRNA}_{\text{m}}^{\text{Arg}}$ s and bacteriophage T4  $\text{tRNA}_{\text{m}}^{\text{Arg}}$  is shown in Fig. 1. Comparison of this composite with the structure of the elongator  $\text{tRNA}_{\text{m}}^{\text{Met}}$  ( $\text{tRNA}_{\text{m}}^{\text{Met}}$ ) reveals that all of the bases conserved in  $\text{tRNA}_{\text{m}}^{\text{Arg}}$ s are present in  $\text{tRNA}_{\text{m}}^{\text{Met}}$  except for the anticodon base C35 and A20 in the dihydrouridine loop. This suggests that one or both of these sites are important for discrimination against  $\text{tRNA}_{\text{m}}^{\text{Met}}$  by *E. coli* ArgRS. McClain and Foss (8) have shown that conversion of A20 to U20 destroys the Arg acceptor identity of the amber suppressor tRNA,  $\text{tRNA}_{\text{m}}^{\text{Arg}}$  (CUA), and that substitution of A20 + A59 into  $\text{tRNA}_{\text{m}}^{\text{Phe}}$  (CUA) leads to insertion of mainly Arg by this tRNA at the site of amber codons in vivo. These elegant genetic experiments have clearly established the role of A20 as a component of Arg identity, but do not take into account the potential effect of C35 on the selection of these tRNA substrates by endogenous aminoacyl-tRNA synthetases or address the relative contribution of A20 and C35 to the efficiency of aminoacylation by ArgRS.

To study the structural basis for the discrimination against  $\text{tRNA}_{\text{m}}^{\text{Met}}$  by ArgRS, we synthesized and assayed a series of  $\text{tRNA}_{\text{m}}^{\text{Met}}$  derivatives. Wild-type and mutant tRNAs were prepared by in vitro transcription with T7 RNA polymerase as described before (2). Such transcripts contain none of the modified bases normally present in native tRNAs, but show near-normal amino acid acceptor activity with cognate aminoacyl-tRNA synthetases and are effectively discriminated against by noncognate enzymes (2, 11, 17–19). As expected, the transcript containing the sequence of wild-type  $\text{tRNA}_{\text{m}}^{\text{Met}}$  (CAU) is efficiently aminoacylated with Met by MetRS, but is a very poor substrate for ArgRS (Table 1). The initial rate of Arg acceptance increases linearly with increasing  $\text{tRNA}_{\text{m}}^{\text{Met}}$  (CAU) up to  $40 \mu\text{M}$ , indicating that this concentration is much less than the Michaelis constant  $K_{\text{m}}$  for the tRNA. Under these conditions, accurate values for the kinetic parameters for Arg acceptance cannot be obtained, but the slope of the linear plot of initial rate versus  $\text{tRNA}_{\text{m}}^{\text{Met}}$  (CAU) concentration gives  $V/K_{\text{m}}$ , where  $V$  is the maximal velocity. Comparison of  $V/K_{\text{m}}$  for the transcripts of  $\text{tRNA}_{\text{m}}^{\text{Arg}}$  (CCG) and  $\text{tRNA}_{\text{m}}^{\text{Met}}$  (CAU) shows that the relative specificity of ArgRS for its cognate tRNA is about seven orders of magnitude greater than that for the noncognate  $\text{tRNA}_{\text{m}}^{\text{Met}}$ . Substitution of A20 for U20 in wild-type  $\text{tRNA}_{\text{m}}^{\text{Met}}$  produces a 1000-fold increase in  $V/K_{\text{m}}$  for Arg acceptance, whereas substitution of the Arg anticodon CCG for the Met anticodon CAU results in a 40,000-fold increase in specificity for ArgRS. A combination of these two changes, yielding

Department of Developmental Biology and Cancer, Albert Einstein College of Medicine, Bronx, NY 10461.

tRNA<sub>m</sub><sup>Met</sup> (CCG) A20, produces a mutant tRNA<sub>m</sub><sup>Met</sup> with near normal Arg acceptor activity (Table 1). These results emphasize the relative importance of the anticodon base C35 in Arg acceptor identity.

Major identity elements have also been found at position 20 and in the anticodon of tRNA<sup>Phe</sup>s from both yeast and *E. coli* (7, 11, 17, 23). In vitro studies on yeast tRNA<sup>Phe</sup> have shown that G20, the anticodon nucleotides G34, A35, and A36, and A73 each contribute approximately equally to Phe identity (11). In contrast, our results show that the contribution of the anticodon CCG to the Arg identity of tRNA<sub>m</sub><sup>Met</sup> is much greater than that of A20. It is possible that

A35 in the Met anticodon may be a strong negative determinant that inhibits interaction of ArgRS with tRNA<sub>m</sub><sup>Met</sup>(CAU) A20 and tRNA<sub>m</sub><sup>Met</sup>(CAU). Such a negative interaction could be required in vivo for complete discrimination against the wild-type tRNA<sup>Met</sup>, which otherwise strongly resembles the natural Arg enzyme substrates.

Previous studies have shown that the anticodon is the major site of recognition of tRNA<sub>m</sub><sup>Met</sup>s by MetRS (2, 10). Indeed, replacement of the wild-type anticodon in tRNA<sub>m</sub><sup>Met</sup> with the Arg anticodon CCG, involving base substitutions at positions 35 and 36, causes a dramatic loss of Met acceptor activity (Table 1).  $V/K_m$  for

tRNA<sub>m</sub><sup>Met</sup> (CCG) is reduced more than four orders of magnitude. The mutant tRNA retains the most important nucleotide for Met identity, C34, and has a  $K_m$  only slightly greater than that observed for tRNA<sub>m</sub><sup>Met</sup> (CAU). Thus, the changes introduced at anticodon bases 35 and 36 largely affect the rate of aminoacylation by MetRS, possibly by interfering with the exact fit required to correctly position the 3' terminus of the tRNA at the active site of the enzyme. Substitution of A20 for U20 has only a small negative effect (two- to threefold) on interaction of tRNA<sub>m</sub><sup>Met</sup> with MetRS (Table 1), consistent with previous studies on tRNA recognition by this enzyme (2, 20–22).

Nucleotide changes in only two locations are sufficient to change the identity of tRNA<sub>m</sub><sup>Met</sup> from Met to Arg. However, additional nucleotides that are also important for recognition by ArgRS may be shared by tRNA<sub>m</sub><sup>Met</sup> and tRNA<sup>Arg</sup>s. The available data suggest that in vivo experiments with opal suppressor tRNA derivatives, which retain C35 in the anticodon, could be productively used to examine the structural features outside of the anticodon that are required for accurate aminoacylation of tRNAs by ArgRS in *E. coli* cells. Indeed, recent experiments from McClain's laboratory indicate that in contrast to the arginine amber suppressor tRNA, tRNA<sup>Arg</sup> containing the opal anticodon inserts only arginine in vivo (26).

**Fig. 1. (Left)** Composite structure of nucleotides common to *E. coli* and bacteriophage T4 tRNA<sup>Arg</sup>s (16). The sequence of tRNA<sub>2</sub><sup>Arg</sup> (ACG) is in question (8) and has been excluded from the composite. Dots indicate positions of sequence variation. Base modifications have been ignored in compiling the conserved sites. Numbering is from the 5' end of the tRNA according to (16). Conserved nucleotides that are not present in tRNA<sub>m</sub><sup>Met</sup> have been boxed. **(Right)** The primary sequence of the transcript of the *E. coli* elongator tRNA<sub>m</sub><sup>Met</sup> (25). Mutations created in the present study are indicated by arrows.

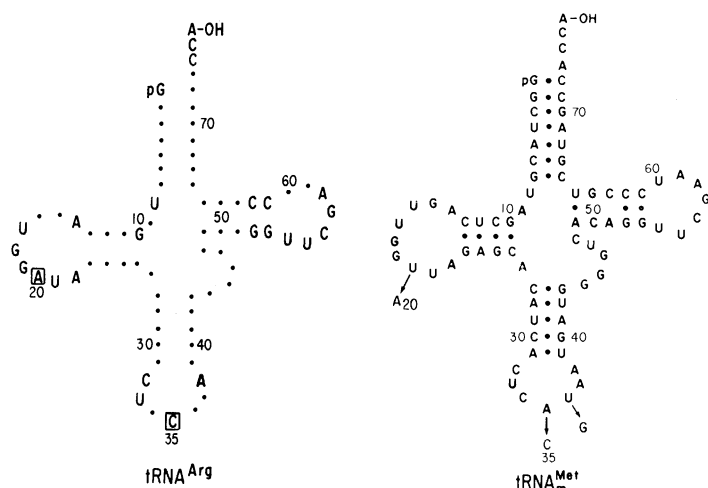


**Table 1.** Kinetic parameters for aminoacylation of tRNAs with *E. coli* ArgRS and MetRS. The tRNA genes were constructed and transcribed as described before (2). The sequence of tRNA<sup>Arg</sup> is that of the major isoacceptor tRNA<sup>Arg</sup> (13), except that the anticodon has been changed from ACG to CCG. Aminoacylation reactions with purified *E. coli* MetRS are as described in (2). For aminoacylation by ArgRS, the specific activity for Arg acceptance of this transcript was 1300 pmol per unit of absorbance at 260 nm ( $A_{260}$ ) and for tRNA<sub>m</sub><sup>Met</sup>(CCG)A20 was 1200 pmol/ $A_{260}$ . Incomplete aminoacylations with ArgRS were observed with the other tRNA<sub>m</sub><sup>Met</sup> derivatives. Specific activities of 1200 pmol/ $A_{260}$  were used to calculate the concentrations of tRNA<sub>m</sub><sup>Met</sup>(CCG) and tRNA<sub>m</sub><sup>Met</sup>(CAU)A20. The specific activity of tRNA<sub>m</sub><sup>Met</sup>(CAU) was taken as 1400 pmol/ $A_{260}$  based on its Met acceptor activity with MetRS. Reaction mixtures for Arg acceptance contained 50 mM tris-HCl, pH 8.0, 0.1 mM EDTA, 4 mM adenosine triphosphate, 10 mM MgCl<sub>2</sub>, 7 μg/ml bovine serum albumin, 0.5 to 40 μM tRNA, and 60 μM [<sup>14</sup>C]arginine (470 cpm/pmol). The *E. coli* ArgRS was partially purified from an overproducing strain (24). Samples were incubated with enzyme at 37°C and treated as described (20).  $K_m$  values are ±20%. Individual kinetic parameters could not be measured for tRNA<sub>m</sub><sup>Met</sup>(CAU) with ArgRS or for tRNA<sub>m</sub><sup>Met</sup>(CCG)A20 with MetRS.

tRNA	$K_m$ (μM)	$V$ (μmol min <sup>-1</sup> mg <sup>-1</sup> )	$V/K_m$	Relative $V/K_m$
<i>Arg-tRNA synthetase</i>				
tRNA <sup>Arg</sup> (CCG)	1.1	2.0	1.8	1 × 10 <sup>7</sup>
tRNA <sub>m</sub> <sup>Met</sup> (CCG)A20	1.2	0.9	0.8	5 × 10 <sup>6</sup>
tRNA <sub>m</sub> <sup>Met</sup> (CCG)	5.2	3 × 10 <sup>-2</sup>	6 × 10 <sup>-3</sup>	4 × 10 <sup>4</sup>
tRNA <sub>m</sub> <sup>Met</sup> (CAU)A20	4.4	7 × 10 <sup>-4</sup>	2 × 10 <sup>-4</sup>	1 × 10 <sup>3</sup>
tRNA <sub>m</sub> <sup>Met</sup> (CAU)			1.5 × 10 <sup>-7</sup>	1
<i>Met-tRNA synthetase</i>				
tRNA <sub>m</sub> <sup>Met</sup> (CAU)	1.1	1.9	1.7	8 × 10 <sup>4</sup>
tRNA <sub>m</sub> <sup>Met</sup> (CAU)A20	1.6	1.5	0.9	4 × 10 <sup>4</sup>
tRNA <sub>m</sub> <sup>Met</sup> (CCG)	2.9	2 × 10 <sup>-4</sup>	7 × 10 <sup>-5</sup>	3
tRNA <sub>m</sub> <sup>Met</sup> (CCG)A20			2 × 10 <sup>-5</sup>	1

#### REFERENCES AND NOTES

1. J. Normanly and J. Abelson, *Annu. Rev. Biochem.* **58**, 1029 (1989).
2. L. H. Schulman and H. Pelka, *Science* **242**, 765 (1988).
3. L. H. Schulman and J. Abelson, *ibid.* **240**, 1591 (1988).
4. Y.-M. Hou and P. R. Schimmel, *Nature* **333**, 140 (1988).
5. W. H. McClain and K. Foss, *Science* **240**, 793 (1988).
6. M. J. Rogers and D. Söll, *Proc. Natl. Acad. Sci. U.S.A.* **85**, 6627 (1988).
7. W. H. McClain and K. Foss, *J. Mol. Biol.* **202**, 697 (1988).
8. ———, *Science* **241**, 1804 (1988).
9. J. Normanly *et al.*, *Nature* **321**, 213 (1986).
10. T. Muramatsu *et al.*, *ibid.* **336**, 179 (1988).
11. J. R. Sampson *et al.*, *Science* **243**, 1363 (1989).
12. L. Kisselev, *Prog. Nucleic Acid Res. Mol. Biol.* **32**, 237 (1985).
13. K. Chakraborty, *Nucleic Acids Res.* **2**, 1793 (1975).
14. ———, *ibid.* **8**, 4459 (1980).
15. J. Ofengand and C. J. Henes, *J. Biol. Chem.* **244**, 6241 (1968).
16. M. Sprinzl *et al.*, *Nucleic Acids Res.* **17**, rl (1989).
17. J. R. Sampson and O. C. Uhlenbeck, *Proc. Natl. Acad. Sci. U.S.A.* **85**, 1033 (1988).
18. T. Samuelsson, T. Boren, T.-I. Johansen, F. Lustig, *J. Biol. Chem.* **263**, 13692 (1988).
19. T. W. Dreher *et al.*, *Nature* **311**, 171 (1984).
20. L. H. Schulman and H. Pelka, *Proc. Natl. Acad. Sci. U.S.A.* **80**, 6755 (1983).
21. L. H. Schulman, in *Transfer RNA: Structure, Properties and Recognition*, P. R. Schimmel, D. Söll, J. Abelson, Eds. (Cold Spring Harbor Laboratory, Cold Spring Harbor, NY 1979), p. 311.
22. ——— and H. Pelka, *Biochemistry* **16**, 4256 (1977).
23. E. F. Tinkle and O. C. Uhlenbeck, unpublished results.

24. F. Neidhardt, V. Vaughn, T. A. Phillips, P. L. Bloch, *Microbiol. Rev.* **47**, 231 (1983).  
 25. S. Cory *et al.*, *Nature* **220**, 1039 (1968).  
 26. W. H. McClain, unpublished results.  
 27. We thank W. H. McClain and O. C. Uhlenbeck for communication of results prior to publication, and B. Bachmann for the overproducing strain of Arg-

tRNA synthetase. Deoxyoligonucleotides were synthesized by a Core facility of Albert Einstein College of Medicine supported in part by National Science Foundation grant PCM-8400114. Supported by American Cancer Society grant NP19R.

13 September 1989; accepted 27 October 1989

## A Model of Human Acute Lymphoblastic Leukemia in Immune-Deficient SCID Mice

SUZANNE KAMEL-REID, MICHELLE LETARTE, CHRISTIAN SIRARD, MONICA DOEDENS, TOM GRUNBERGER, GABRIELLE FULOP, MELVIN H. FREEDMAN, ROBERT A. PHILLIPS, JOHN E. DICK\*

A human acute lymphoblastic leukemia (ALL) cell line that was transplanted into immune-deficient SCID mice proliferated in the hematopoietic tissues, invaded various organs, and led to the death of the mice. The distribution of leukemic cells in SCID mice was similar to the course of the disease in children. A-1 cells marked with a retrovirus vector showed clonal evolution after the transplant. SCID mice that were injected with bone marrow from three patients with non-T ALL had leukemic cells in their bone marrow and spleen. This *in vivo* model of human leukemia is an approach to understanding leukemic growth and progression and is a novel system for testing new treatment strategies.

MUCH PROGRESS HAS BEEN MADE recently in identifying regulatory genes involved in cell development and maturation by studying the genetic changes of transformed cells in both *in vitro* and *in vivo* model systems. Such models are not available for human leukemic cells, especially childhood acute leukemias. The difficulties in culturing primary human leukemic cells suggest that selective processes may alter the properties of such cells over time (1). *In vivo* models would aid in the development of treatment strategies and further our understanding of leukemic transformation and progression. Subcutaneous transplantation of lymphoid and myeloid cell lines (2-9), lymphomas (8), or primary patient material (2) into nude mice produces myelomas or localized solid tumors (10) uncharacteristic of the primary leukemia. The growth of one human leukemia cell line in the hematopoietic tissues of nude mice has been described (11). This cell line

was an aneuploid T ALL originally established and maintained as an ascites tumor in nude mice; the animals died within 2 to 4 weeks. However, growth as an ascites does not reflect the normal course of the disease

in children. We, therefore, developed an experimental system in which the growth of human leukemic cells in murine hematopoietic tissues was more analogous to growth in patients with leukemia.

Non-T ALL is the most prevalent childhood leukemia and is characterized by a pre-B cell phenotype (12). A cell line (A-1) was established from the peripheral blood of a patient undergoing a terminal relapse of non-T ALL (13). The A-1 cells were HLA-DR<sup>+</sup>, CD19<sup>+</sup>, CALLA<sup>-</sup> (CD10), and CD20<sup>-</sup>. No cytoplasmic or surface immunoglobulin was detected; it has one rearranged  $\mu$  chain gene and unrearranged light chain genes, characteristic of a pre-B cell line (13). The A-1 line was EBV free, had a normal karyotype, and grew autonomously producing an unidentified factor (not interleukin-1, -2, -3, -4, -5, -6, granulocyte-, or granulocyte/macrophage-colony stimulating factor) that augmented its growth in semisolid and suspension cultures.

Normal human hematopoietic cells (14-16) and human tumors (17) can be engrafted into immune-deficient SCID (18) or *bg/nu/xid* (19) mice; thus, they may be better recipients than nude mice for the transplantation of human leukemic cells. Immune-deficient SCID and *bg/nu/xid* mice differ in their ability to be engrafted with normal human bone marrow; *bg/nu/xid* mice con-

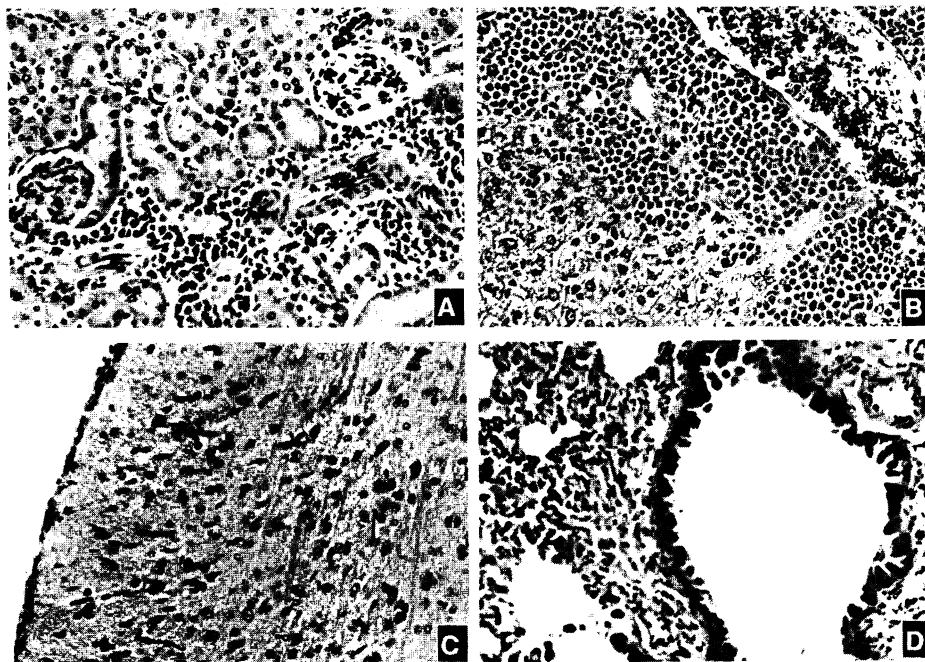


**Fig. 1.** Histological analysis of SCID mice 8 weeks after transplantation with the A-1 leukemic cells. Tissue sections were obtained from the kidney (A), liver (B), brain (C), and lung (D) of SCID mice transplanted with A-1 cells. The tissues were fixed in 10% formalin, paraffin embedded, and 4  $\mu$ m sections were cut and stained with hematoxylin and eosin. Microscopic evaluation indicated that there was a light leukemic infiltration in the interstitial region between the tubules in the kidney (A) and in the periportal regions of the liver (B). Note the normal hepatocytes in the lower left hand corner of (B). No leukemic cells were observed in the cerebral cortex or meninges of the brain (C) or in the peribronchial region of the lung (D). Magnification is  $\times 40$ .

S. Kamel-Reid, C. Sirard, M. Doedens, J. E. Dick, Department of Genetics, Research Institute, Hospital for Sick Children, and Department of Medical Genetics, University of Toronto, Toronto, Ontario M5G 1X8.  
 M. Letarte, Department of Immunology, Hospital for Sick Children, Toronto, and Department of Immunology, University of Toronto.

T. Grunberger, G. Fulop, M. H. Freedman, Division of Hematology/Oncology, Research Institute, Hospital for Sick Children, and Department of Pediatrics, University of Toronto.

R. A. Phillips, Division of Hematology/Oncology, Research Institute, Hospital for Sick Children, and Departments of Immunology and Medical Genetics, University of Toronto.

\*To whom correspondence should be addressed.